AGU PUBLICATIONS

Earth's Future

RESEARCH ARTICLE

10.1002/2015EF000336

# Uncertainty partition challenges the predictability of vital details of climate change

**Simone Fatichi[1], Valeriy Y. Ivanov[2], Athanasios Paschalis[3,4], Nadav Peleg[1], Peter Molnar[1], Stefan Rimkus[1,5], Jongho Kim[2,6], Paolo Burlando[1], and Enrica Caporali[7]**

[1]Institute of Environmental Engineering, ETH Zurich, Zurich, Switzerland, [2]Department of Civil and Environmental Engineering, University of Michigan, Ann Arbor, Michigan, USA, [3]Faculty of Engineering and the Environment, University of Southampton, Southampton, UK, [4]Nicholas School of the Environment, Duke University, Durham, North Carolina, USA, [5]SCOR Global P&C, Zurich, Switzerland, [6]Department of Civil and Environmental Engineering, Sejong University, Seoul, Republic of Korea, [7]Department of Civil and Environmental Engineering, University of Firenze, Firenze, Italy

**Key Points:**
- Uncertainties of climate change projections at high spatial and temporal resolution are analyzed
- Uncertainty cannot be reduced in precipitation projections and for extremes
- Uncertainty in air temperature can be potentially constrained with refined emission scenarios

**Supporting Information:**
- Supporting Information S1

**Corresponding author:**
S. Fatichi, simone.fatichi@ifu.baug.ethz.ch

**Citation:**
Fatichi, S., V. Y. Ivanov, A. Paschalis, N. Peleg, P. Molnar, S. Rimkus, J. Kim, P. Burlando, and E. Caporali (2016), Uncertainty partition challenges the predictability of vital details of climate change, *Earth's Future*, *4*, 240–251, doi:10.1002/2015EF000336.

Received 8 NOV 2015
Accepted 21 APR 2016
Accepted article online 29 APR 2016
Published online 20 MAY 2016



**Abstract** Decision makers and consultants are particularly interested in "detailed" information on future climate to prepare adaptation strategies and adjust design criteria. Projections of future climate at local spatial scales and fine temporal resolutions are subject to the same uncertainties as those at the global scale but the partition among uncertainty sources (emission scenarios, climate models, and internal climate variability) remains largely unquantified. At the local scale, the uncertainty of the mean and extremes of precipitation is shown to be irreducible for mid and end-of-century projections because it is almost entirely caused by internal climate variability (stochasticity). Conversely, projected changes in mean air temperature and other meteorological variables can be largely constrained, even at local scales, if more accurate emission scenarios can be developed. The results were obtained by applying a comprehensive stochastic downscaling technique to climate model outputs for three exemplary locations. In contrast with earlier studies, the three sources of uncertainty are considered as dependent and, therefore, non-additive. The evidence of the predominant role of internal climate variability leaves little room for uncertainty reduction in precipitation projections; however, the inference is not necessarily negative, because the uncertainty of historic observations is almost as large as that for future projections with direct implications for climate change adaptation measures.

## 1. Introduction

Impact studies demand meteorological forcing at local spatial scales and fine temporal resolutions referred by *Kerr* [2011] as "vital details" of climate change. Yet robust projections at scales commensurate with practical applications and for extremes [*Maraun et al.*, 2010] are still unavailable as climate model results are typically more reliable in terms of mean values and averaged globally or for large regions [*Kendon et al.*, 2012; *Knutti and Sedláček*, 2013; *Xie et al.*, 2015]. Uncertainties in climate change projections are very large [*Murphy et al.*, 2004; *Knutti*, 2008; *Maslin and Austin*, 2012]. However, a better knowledge of the relative contribution of the three main sources, anthropogenic forcing (scenario uncertainty), climate model (model epistemic uncertainty), and internal climate variability (stochastic uncertainty), is important for understanding how much of the overall uncertainty can be decreased through improvements of current climate models and/or emission scenarios [*Cox and Stephenson*, 2007; *Deser et al.*, 2012a; *Fischer et al.*, 2013], or will remain irreducible in the form of internal variability. Previous studies presented computations of signal to noise ratio in climate change projections [*Giorgi and Bi*, 2009; *Santer et al.*, 2011; *Hawkins and Sutton*, 2012; *Deser et al.*, 2014], or directly partitioned uncertainty into its different sources, subject to the simplified assumption of the independence among the sources [*Hawkins and Sutton*, 2009, 2011; *Hingray and Saïd*, 2014; *Little et al.*, 2015]. At the global and regional scales, the scenario uncertainty has been found to be the primary source for air temperature projections. Model uncertainty has been argued to dominate sea level rise and precipitation projections, especially when internal climate variability becomes less relevant for longer lead-time projections because of stronger climate change signals [*Hawkins and Sutton*, 2011; *Little et al.*, 2015]. Studies at regional scale nonetheless indicate that internal climate variability for precipitation projections can exceed 50% of the total uncertainty, lasting throughout the end of this century [*Hingray and Saïd*, 2014]. Previous studies targeted temporal (>hours) and spatial (>hundreds of kilometers) scales that

do not correspond to the typical scales at which adaptation strategies are undertaken. While from theory we know that the uncertainty related to internal climate variability is progressively more important as spatial and temporal scales decrease [*Giorgi*, 2002], there has been no research on its contribution to the uncertainty of climate change projections at the scales that are most relevant for impact studies. This knowledge gap is addressed in this study.

Here, for each location we generate 20,200, 30-year long realizations of probable future climates at the local (station) scale, 10,100 for mid-century (2046–2065) and 10,100 for end-of-the-century (2081–2100), using a stochastic downscaling technique that combines an hourly weather generator Advanced WEather GENerator (AWE-GEN) [*Fatichi et al.*, 2011] and a Bayesian methodology [*Tebaldi et al.*, 2005; *Fatichi et al.*, 2013]. We compute factors of change (FC) from simulations of 32 climate models used in the Coupled Model Intercomparison Project Phase 5 (CMIP5) for two different emission scenarios (RCP 4.5 and RCP 8.5). This approach allows us to generate ensembles of future climate projections at the hourly time scale for different meteorological variables (precipitation, air temperature, relative humidity, and shortwave radiation) at three selected locations, representative examples of considerably different climate conditions: Zurich (Switzerland), Miami, and San Francisco (USA). Specifically, the three main sources of uncertainty: climate model (epistemic uncertainty), anthropogenic forcing (scenario uncertainty), and climate internal variability (stochastic uncertainty) are partitioned considering them as dependent, i.e., accounting for the possible co-variance among the uncertainty sources, in contrast to several previous studies at global and regional scales [*Hawkins and Sutton*, 2009, 2011; *Yip et al.*, 2011; *Rowell*, 2012; *Orlowsky and Seneviratne*, 2013; *Hingray and Saïd*, 2014; *Little et al.*, 2015]. The sum of the individual variances is therefore expected to be larger (for negative correlations) or smaller (for positive correlations) than the variance corresponding to the sum of the three uncertainty sources (i.e., the total uncertainty), depending on the degree of actual co-variation. If uncertainty is expressed in terms of a percentile range, this range can be also different from the range expected from independent variables.

## 2. Methods

### 2.1. Locations

Three locations were selected for this analysis: Zurich (8.56°E 47.38°N; elevation 555 m a.s.l.), Switzerland, San Francisco (122.39°W 37.62°N; elevation 27 m a.s.l.), and Miami (80.28°W 25.91°N; elevation 56 m a.s.l.), USA. Meteorological data were obtained from quality-controlled weather stations covering 30-year periods, 1981–2010 for Zurich, and 1961–1990 for San Francisco and Miami. Precipitation data for Switzerland were provided by MeteoSwiss, the Federal Office of Meteorology and Climatology and for the United States from WebMET (http://www.webmet.com/). Hourly precipitation, air temperature, shortwave radiation, and relative humidity were available for the entire period with limited gaps (<0.1%). The three locations were selected because of their different climate characteristics (Supporting Information, Figure S1). Zurich presents pre-alpine climate with humid summer and relatively cold winter, the average precipitation is 1124 mm $year^{-1}$, and the mean temperature is 9.4°C (1981–2010). It is classified as humid continental climate according to Köppen–Geiger (KG) climatology [*Peel et al.*, 2007]. San Francisco climate exhibits Mediterranean precipitation regime with dry summers and wet winters but small seasonality of air temperature (cool-summer Mediterranean climate according to KG classification). The average precipitation is 501 mm $year^{-1}$ and the mean temperature is 13.3°C (1961–1990). Miami has sub-tropical climate with warm temperatures throughout the year, receiving a relatively high amount of precipitation especially during summer (Tropical monsoon climate according to KG classification). The average precipitation is 1423 mm $year^{-1}$ and the mean temperature is 24.2°C (1961–1990).

### 2.2. Climate Models

Daily model runs for 32 General Circulation Models (GCMs) were obtained from the dataset compiled in the World Climate Research Programme's (WCRP's), CMIP5 [*Taylor et al.*, 2012]. Specifically, climate models that were used in this work are listed in the Supporting Information, Table S1. We used model simulations driven with historical forcing until 2005 and the emission scenarios RCP4.5 and RCP8.5 until 2100 [*Moss et al.*, 2010]. Scenarios RCP2.6 and RCP6.0 were not used because daily simulations required for the downscaling approach were available only for a limited number of models.

### 2.3. Weather Generator

The AWE-GEN is a stochastic simulator that generates hourly time series of weather variables (precipitation, cloud cover, air temperature, incoming shortwave radiation, wind speed, and atmospheric pressure) for a given stationary climate [*Ivanov et al*., 2007; *Fatichi et al*., 2011]. The model parameters are estimated using station level observations. Precipitation is the primary driving variable and it is simulated using the Neyman–Scott rectangular pulse model [*Cowpertwait et al*., 2007; *Paschalis et al*., 2014]. Model parameters are month specific to preserve seasonality. Interannual dynamics are imposed by simulating annual precipitation using a first order autoregressive model [*Fatichi et al*., 2011]. Cloud cover evolution is simulated as a smooth transition between complete cloud cover during storms and partial or absent cloud cover during "fair-weather" periods [*Ivanov et al*., 2007]. Air temperature, vapor pressure, and wind speed are simulated using a combination of deterministic components, which introduce dependencies among meteorological variables (e.g., between rainy hours and cloud cover, changes in air temperature and sun position, solar radiation and wind speed, etc.), and high frequency (1-h) stochastic components. Shortwave radiation is simulated with a two-band atmospheric radiation transfer model for clear sky conditions [*Gueymard*, 2008], modified to account for cloud cover [*Stephens*, 1978; *Slingo*, 1989]. For a complete description of the AWE-GEN model structure and parameterization, the reader is referred to *Fatichi et al*. [2011] and to the AWE-GEN technical reference (http://www-personal.umich.edu/ivanov/HYDROWIT/Models.html). Performance of AWE-GEN for Zurich, San Francisco, and Miami was comparable to previously presented results [e.g., *Fatichi et al*., 2011] and was highly satisfactory in simulating the statistics of the observed climate. Note that the combination of deterministic and stochastic components allows AWE-GEN to preserve to a large extent physical realism in the co-variance between meteorological variables unlike many other weather generators [e.g., *Bordoy and Burlando*, 2014], for instance temperature, relative humidity, shortwave radiation statistics are considerably different in rainy and non-rainy days.

### 2.4. Stochastic Downscaling

A stochastic downscaling approach is used to generate 20,200, 30-year long, hourly time series of meteorological variables for each of the three locations (Table 1). These simulations represent a set of possible conditions obtained by permutating 2 future climate periods, 101 climate model trajectories, 2 emission scenarios, and 50 stochastic realizations. The stochastic downscaling uses simulations from climate models and the hourly weather generator AWE-GEN. Detailed procedural steps, mathematical formulation and assumptions of the methodology for generating the hourly time series of future scenarios are described in *Fatichi et al*. [2011, 2013]. Improvements have been applied to the original methodology, and are outlined below along with a summary of the overall procedure.

Information for projected climate change is derived from simulations of GCMs. Based on GCM statistics for a historic and future periods, we compute "FC", which are either additive (for air temperature) or multiplicative (for precipitation) (see an extensive review by *Anandhi et al*. [2011]). Specifically, time series of daily precipitation and monthly temperature are used for estimation of daily, monthly, and annual statistics. Statistics are computed for a representative period corresponding to the years for which observations are available (historic) and two future periods: mid-century (2046–2065) and end-of-the-century (2081–2100). Note that even though climate change signals are estimated from a 20-year period, 30-year long time series are generated with AWE-GEN for each future trajectory, with 30-year period being a typical interval used to define climatological values according to the World Meteorological Organization. The historic and future periods are assumed stationary to estimate the statistics.

**Table 1.** A List of the Permutation Scenarios Used to Generate the 20,200, 30-Year Long, Hourly Time Series of Meteorological Variables for Each of the Three Locations

| | Mid-Century (2046–2065) | End-Century (2081–2100) |
|---|---|---|
| Scenario uncertainty | 2 | 2 |
| Climate model uncertainty | 100 + 1 (Median) | 100 + 1 (Median) |
| Stochastic uncertainty | 50 | 50 |
| Total uncertainty | 10,100 | 10,100 |

We extract the long-term means for each month from air temperature time series. For precipitation, we estimate the mean, the variance, and the frequency of non-precipitation for different aggregation intervals (24, 48, 72, and 96 h), that is three statistics for four aggregation intervals over 12-month annual cycle. In addition to account for low-frequency properties of the precipitation process, the coefficient of variation of annual precipitation is estimated. In order to compute the parameters of the precipitation module of AWE-GEN, additional statistics of precipitation such as lag-1 autocorrelation and skewness are required along with an extension of all precipitation statistics to the hourly time scale. The extension from daily or larger aggregation time periods ($\geq$24 h) to sub-daily scales ($<$24 and $\geq$1 h) is discussed in *Fatichi et al.* [2011, 2013]. In this study, we present the uncertainty of estimation of each precipitation statistic at the aggregation periods utilized in the weather generator (1, 6, 24, and 72 h) using 30-year long time series (Figure S2). Specifically, the uncertainty bars of the statistics ($\pm$1 standard deviation) are computed with two methods: (i) bootstrapping 100 times individual years with repetition from the observed climate time series, (ii) simulating 100 times 30 years of historic climate using AWE-GEN. The results are identical for the two methods except for small deviations in terms of estimation of lag-1 autocorrelation and skewness at the aggregation periods larger than one day. This outcome strongly reinforces the credibility of the weather generator that realistically reproduces internal climate variability over the analyzed period and shows that several statistics of precipitation are uncertain, even when they are computed from 30 years of data.

Uncertainty in the historic climate statistics is presented in terms of "FC", i.e., it is normalized with respect to the expected value in order to have a direct comparison between observational uncertainty and potential climate change signals. Using 30 years of data, monthly mean precipitation is known with an accuracy of $\pm$10% (FC = 0.9 – 1.1), while the variance statistics are less accurate $\pm$20% (FC = 0.82 – 1.18). The largest uncertainties concern the computation of lag-1 autocorrelation and skewness, while the frequency of non-precipitation is almost perfectly determined (FC = 0.98 – 1.02). Given the large uncertainties (>30%) in the estimation of the lag-1 autocorrelation and skewness for historic climate for aggregation periods larger than 1 h, contrary to our previous studies [*Fatichi et al*., 2011, 2013; *Caracciolo et al*., 2014; *Francipane et al*., 2015; *Kim and Ivanov*, 2015], we did not attempt to compute FC for these statistics from climate model simulations. We sample their corresponding FC from a uniform distribution constrained by $\pm$1 standard deviation of the expected value of the statistic computed with the analysis of the historic climate. This method gives a plausible estimate of a climate change signal, which would remain impossible to compute exactly, even in the presence of actual future data, because of the estimation uncertainty illustrated in Figure S2. This approach allows us to account for changes in these statistics in the future without their precise knowledge. The alternative of assuming FC = 1, and allowing only for stochastic variability will likely result in a small range of values for these statistics in the future and in an artificial enhancement of the fraction of uncertainty contributed by internal climate variability, because the climate model signal would be removed.

Factors of changes from different GCMs are weighted using a Bayesian methodology [*Tebaldi et al*., 2004, 2005; *Fatichi et al*., 2013] to obtain probability distributions for the FC. This methodology weights equally or unequally different members of the GCM ensemble and produces a numerical representation of the probability distribution function for each FC. In this study, we give an equal weight to each model to avoid introducing another degree of freedom, because robust methodologies to weight models are difficult to define [*Christensen et al*., 2010; *Knutti et al*., 2010; *Weigel et al*., 2010]. Furthermore, differences between weighting techniques are not fundamental determinants of the climate change signals as shown in *Fatichi et al*. [2013]. Another issue, which has been often raised in constructing multi-model ensembles, is related to the relative interdependence among models [*Pennell and Reichler*, 2010; *Masson and Knutti*, 2011; *Knutti et al*., 2013]. Bayesian weighting techniques assume that each model is independent, which is known not to be the case. In our analysis, we used the maximum number of available models (32 models) but we also checked the effect of using a sub-sample of models selecting only one model for each contributing group (19 models) or a random selection of 12 models repeated 20 times (Figures S3 and S4). Using one model per family gives a very similar median and a slightly larger range of variability (10–90 percentile range) of the FC in comparison to using the entire ensemble. The medians typically differ by less than 0.2°C for changes in air temperature, and less than 0.04 for the FC of precipitation. The ranges averaged over the 12 months are 43% larger than using 32 models. Using 12 random models may shift considerably the median of the FC distribution up to 0.8°C and 0.1 for air temperature and precipitation FC, respectively, and affects the

spread of the distribution. The larger spread is expected when using a smaller ensemble but the medians of all variables are reasonably estimated in most of the cases also using a 12-model ensemble. In other words, insofar as the Bayesian weighting method [*Tebaldi et al*., 2004, 2005] is accepted, the computation of "climate model uncertainty" is a robust finding, which is only influenced to a minor extent by the choice of the specific models.

A Sobol quasi-random low discrepancy sequence [*Sobol*, 1976; *Saltelli et al*., 2000], rather than a pure random number generator is used to sample the FC from their respective marginal probability distributions, assuming specific cross-correlations among the FC as done in *Fatichi et al*. [2013]. The Sobol sequence allows a better coverage of the multi-dimensional space of the FC distribution [*Saltelli et al*., 2000; *Pappas et al*., 2013] with a smaller sample size. In this study, 100 + 1 sets of FC are drawn to sample the frequency distributions of projected future climate statistics, with the last 101st sampling designed to provide the median change. Such a large ensemble is used to cover the climate model uncertainty because of variability in FC among individual GCMs and it is sufficient to approximate the 5–95 percentile range of the distribution [*Kim et al*., 2016]. Subsequently, the FC are applied to the climate statistics derived from historical observations to re-evaluate the parameters of the weather generator. In this study, 404 (101 trajectories × 2 future periods × 2 emission scenarios) parameter sets for AWE-GEN were computed, each corresponding to a potential future climate "alternative".

The final step of the methodology is the generation of hourly time series using the re-evaluated parameter sets. An ensemble of 50, 30-year long, hourly time series of meteorological variables was simulated with AWE-GEN for each of the 404 parameter sets, leading to 20,200 simulations for each location. Fifty members have been tested to be a number large enough to approximate the 5–95 percentile range of the stochastic uncertainty [*Kim et al*., 2016].

### 2.5. Uncertainty Partition

The climate model uncertainty is computed separately for the two future periods and the two emission scenarios. We first compute the median of a given variable from the 50 stochastic simulations for each of the 100 future trajectories (climate alternatives), and then we compute the 5–95th percentiles of the obtained values (Figure 1). To estimate the total climate model uncertainty for a given future period, we average the 5–95th percentile ranges obtained for the two emission scenarios RCP4.5 and RCP8.5.

The internal climate variability (stochastic uncertainty) is also computed separately for the two future periods and the two emission scenarios. We take future trajectory corresponding to the median climate change (101st simulation) and estimate the 5–95th percentiles of the corresponding 50 stochastic simulations for a given variable (Figure 1). Similar to the climate model uncertainty, in order to obtain the total stochastic

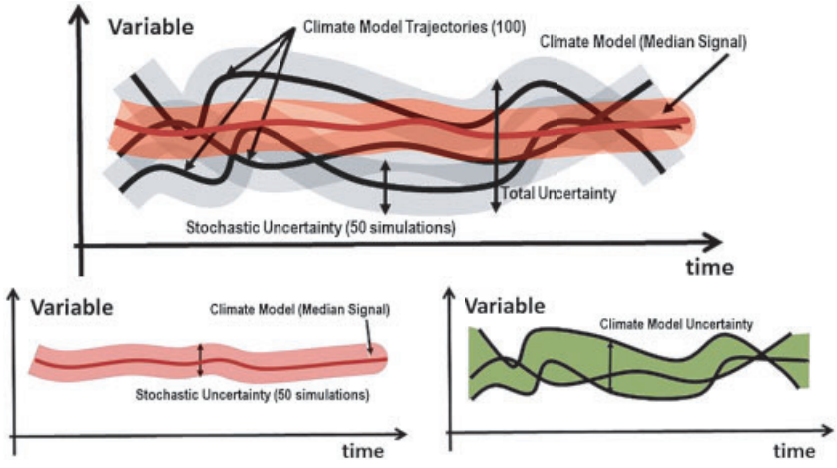


**Figure 1.** A scheme illustrating how different uncertainty types are partitioned in the stochastic downscaling approach. For simplicity, the figure refers only to one future emission scenario and one projection period. Envelopes for climate model and stochastic uncertainties include the entire uncertainty range; in practice, the 5–95th percentile ranges are used.

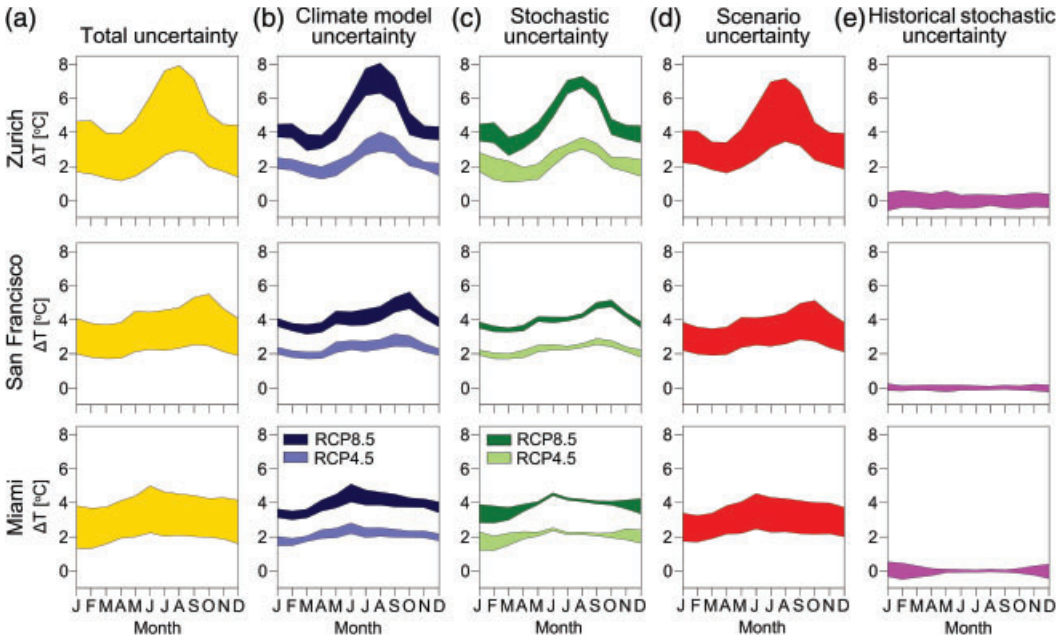


**Figure 2.** Changes in mean monthly air temperature ($\Delta T$ in °C) detected with the stochastic downscaling approach for the period of 2081–2100 with respect to the observational periods for Zurich, San Francisco, and Miami. The colored areas represent the 5th-to-95th percentile ranges of the projections. Different uncertainty types are presented: (a) total uncertainty; (b) climate model uncertainty; (c) stochastic uncertainty (internal variability); (d) emission scenario uncertainty, and (e) historic stochastic uncertainty. In (b) and (c), the results for the two emission scenarios (RCP4.5 and RCP8.5) are presented separately.

uncertainty for a future period, we average the 5–95th percentile ranges obtained for the two emission scenarios RCP4.5 and RCP8.5.

The emission scenario uncertainty is computed for each future period as the difference, for a given variable, between the median of the 5000 ($100 \times 50$) simulations corresponding to RCP8.5 scenario and the median of the 5000 simulations corresponding to the RCP4.5 scenario. The availability of only two emission scenarios forces us to approximate the 5–95th percentile range with the difference between the two end-members. While this represents an approximation of the percentile range statistic, it is an unavoidable assumption, which would be required even if all of the four existing emission scenarios could have been used.

The total uncertainty is computed as the 5–95th percentile range for a given variable for the 10,000 ($100 \times 50 \times 2$) simulations carried out for a given location and future period (Figure 1). Note that while, we refer in the text to total uncertainty, this represents only our best approximation of the "true" total uncertainty, which is forcefully unknown.

Fractional uncertainties are computed by normalizing the 5–95th percentile range of uncertainty of each type (climate model, stochastic, and emission scenario) by the total uncertainty. For instance, for the monthly mean precipitation or mean temperature, these uncertainties correspond to the sum of the differences between the 95th and 5th percentiles for each uncertainty type over 12 months (colored area in Figures 2 and 3).

### 2.6. Uncertainty Co-Variance

For the variance statistic, the sum of the variances of $n$ independent (uncorrelated) random variables is equal to the variance of the sum of these variables [*Papoulis*, 1991]. For positively/negatively correlated random variables the sum of the variances is smaller/larger than the variance of the sum of the variables. Therefore, a comparison between the sum of the variances and the variance of the sum allows one to examine the degree of co-variation (interactions) among the examined variables. Unfortunately, variances cannot be computed for all the three uncertainty sources, because only two values are available to compute emission scenario uncertainty. For the same reason a formal analysis of variance cannot be applied and an alternative solution must be sought.

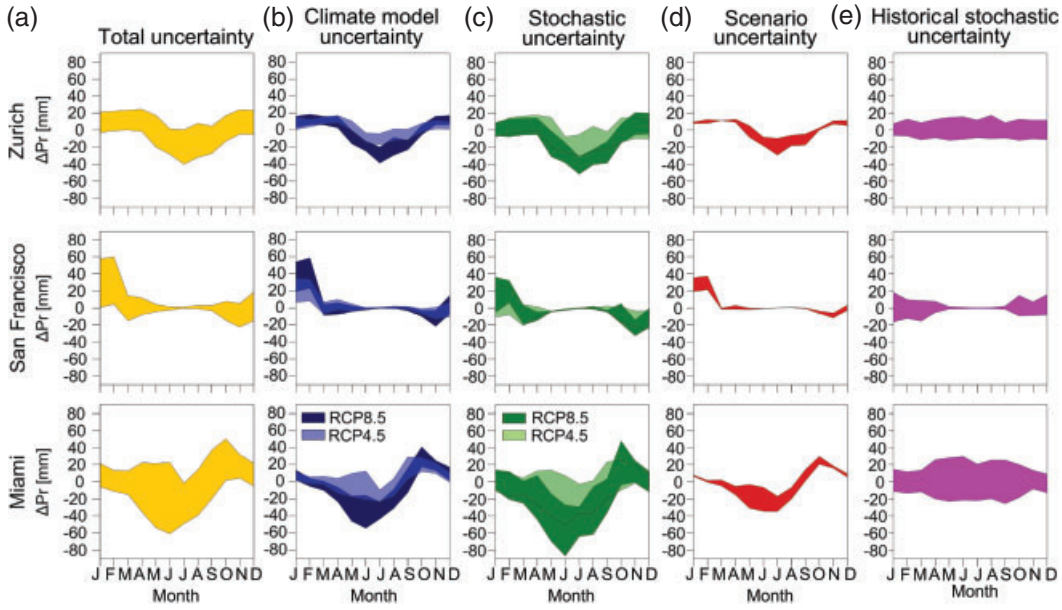


**Figure 3.** Changes in mean monthly precipitation (ΔPr in mm) detected with the stochastic downscaling approach for the period 2081–2100 with respect to the observational period for Zurich, San Francisco, and Miami. The colored areas represent the 5th and 95th percentiles of the projections. Different uncertainty types are presented: (a) total uncertainty; (b) climate model uncertainty; (c) stochastic uncertainty (internal variability); (d) emission scenario uncertainty, and (e) historic stochastic uncertainty. In (b) and (c), the results for the two emission scenarios (RCP4.5 and RCP8.5) are presented separately.

For a given range of percentiles, there is not a general theory that permits defining the ratio between the sum of the percentile range of $n$ independent random variables and the percentile range of the sum of the variables (total uncertainty). This ratio is a function of the number of random variables, the probability distribution of the random variables, and of the parameters of the distributions. For our specific case, we use a Monte Carlo approach to compute numerically this ratio for the 5–95th percentile range for $n = 3$, as three are the uncertainty types we analyzed. We compute the ratio with five distributions (Figure S5). We use three theoretical distributions, a standard normal distribution $N(0,1)$, a uniform distribution between 0 and 1, an exponential distribution with the mean equal to 1, and two combinations of empirical distributions corresponding to the distributions computed for the three uncertainty types for mean temperature and precipitation (Zurich, mid-century period). The ratios between the sum of the percentile ranges of three independent random variables and the percentile range of the sum of three variables are between 1.6 and 2.1 varying across distributions, with the larger values computed from the empirical distributions. In an analogy with the variance, if the ratio between the sum of the percentile ranges and the percentile range of the sum is larger/smaller, than the one expected from independent variables (Figure S5), the variables are negatively/positively correlated.

## 3. Results

Changes in monthly air temperature by the end-of-the-century (2081–2100) for all three analyzed locations show a substantial warming throughout the entire year, more pronounced during summer, especially for Zurich (Figure 2). The total uncertainty (5–95th percentile range) for most of the months is roughly constrained to within 2.5°C, with the striking exception of the summer months in Zurich. The climate change signal, i.e., the distance from zero, is large enough that the lower uncertainty bounds never cross the +1°C line (Figures 2a–2d). Climate model and stochastic uncertainties are presented separately for the two emission scenarios; the difference between the two is representing the scenario uncertainty. As seen, the emission scenario has a large effect on air temperature also at the local scale, with the scenario uncertainty incorporating the largest fraction of the total uncertainty (Figure 2). For reference, we also computed the uncertainty caused by internal variability for the historic climate, which represents the confidence interval for the 30-year mean monthly temperature (see also Figure S2). The historic internal variability is seasonally centered around zero (no change signal) and generally constrained to less than 1°C. A similar

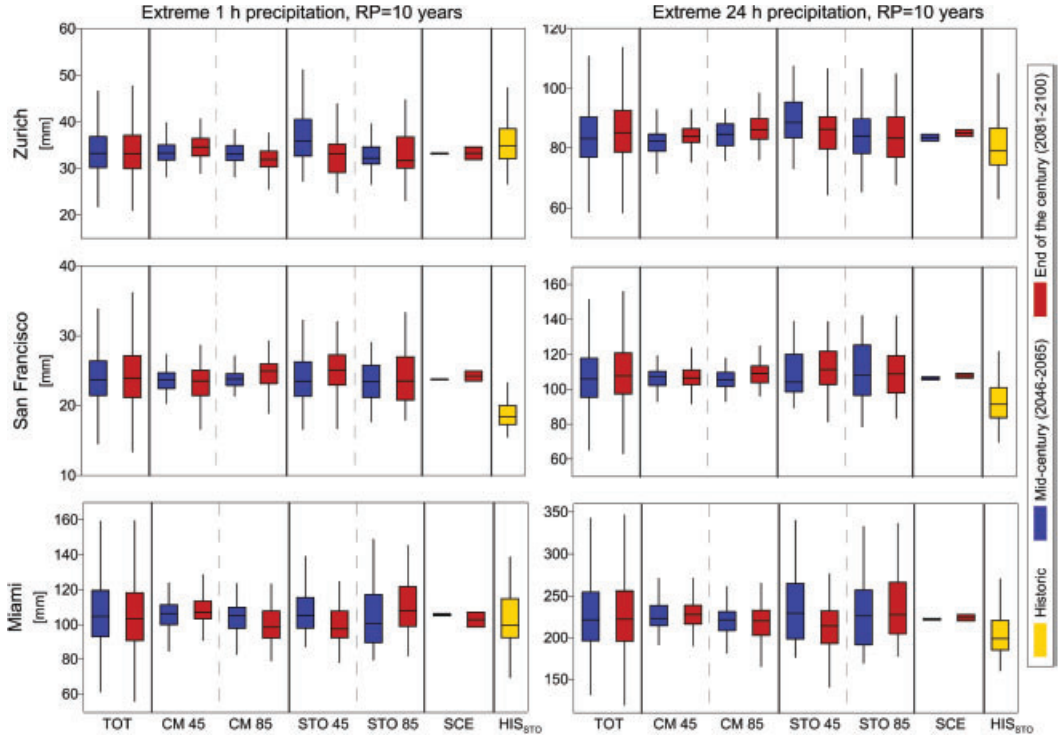


**Figure 4.** Boxplot of simulated extreme 1-h (left panel) and 24-h (right panel) precipitation for a 10-year return period for Zurich, San Francisco, and Miami. The central mark of each box is the median, the edges are the 25th and 75th percentiles, the whiskers extend to the most extreme data points that are not considered outliers. Blue boxplots refer to the projections for mid-century (2046–2065), red boxplots refer to the end-of-the century (2081–2100), and yellow to the historic period. Different uncertainty types are presented: total uncertainty (TOT); climate model uncertainty separately for the two emission scenarios (CM-45 and CM-85); internal climate variability (stochastic uncertainty) separately for the two emission scenarios (STO-45 and STO-85); emission scenario uncertainty (SCE); and historic stochastic uncertainty ($HIS_{STO}$).

range applies to the stochastic uncertainty for the future conditions but centered on the mean climate change signal. The uncertainty due to climate model differences is only slightly larger than the stochastic uncertainty.

Changes in monthly precipitation at the end-of-the-century (2081–2100) show that the total uncertainty can be as large as 40–80 mm (30–60% of the mean) for individual months, with the zero change mostly embedded within the uncertainty envelope (5–95 percentile) for essentially each month and location (Figure 3). The uncertainty range lower than 15 mm (but corresponding to >100% change) for San Francisco during the summer months simply reflects the very low mean precipitation during this season (Figure S1). Climate model and stochastic uncertainties are clearly the major sources for mean precipitation, with the stochastic uncertainty the largest among the two and comparable to the total uncertainty. Not surprisingly, the projections are different for the three locations. However, the relative magnitudes of the uncertainty sources are remarkably invariant despite climatological differences among the three locations. Using the uncertainty caused by internal variability for historic climate as a reference (Figure 3e), it can be seen that it is generally high, i.e., it spans a large fraction of the total uncertainty for the projected future climate conditions (Figure 3).

The dominance of stochastic uncertainty is even more evident when "vital details" of climate change are analyzed (i.e., extreme precipitation at the hourly and daily scales). For the 1- and 24-h extreme precipitation with a return period of 10 years, the scenario and climate model uncertainties become even less relevant, and the total uncertainty can be mostly explained by the internal variability (Figure 4). This does not necessarily imply that the medians for future projections are identical to that of the historic climate, as can be appreciated from the relative differences of the 24-h median extremes for mid- and end-of-the century periods, when compared with historic climate. Present-day stochastic uncertainty is very large, as supported by analysis of long rainfall time series [*Marani and Zanetti*, 2015], and can cover a wide range of possible future climates in terms of local precipitation extremes.

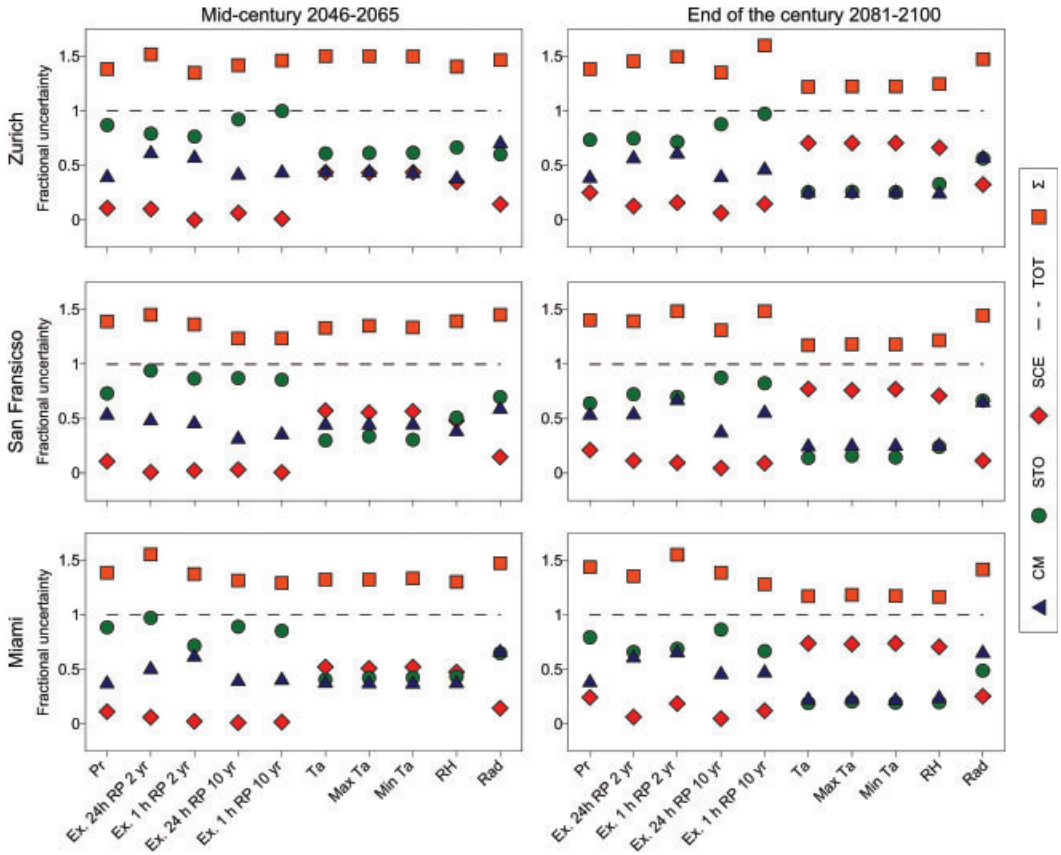


**Figure 5.** The fractional uncertainties for the mid-century (2046–2065), and end-of-the century (2081–2100) projections (left and right panel) for Zurich, San Francisco, and Miami. Different uncertainty sources are presented: climate model uncertainty (CM); internal climate variability (stochastic uncertainty, STO); emission scenario uncertainty (SCE); total uncertainty (TOT); and Σ, the arithmetic sum: $\Sigma = CM + STP + SCE$. The fractional uncertainty is presented for mean precipitation (Pr), extreme precipitation for 24 and 1 h for 2- and 10-year return periods (Ex. 24 h Rp 2 year, Ex. 1 h Rp 2 year, Ex. 24 h Rp 10 year, Ex. 1 h Rp 10 year), mean temperature (Ta), maximum and minimum daily temperature (Max Ta, Min Ta), mean relative humidity (RH), and mean shortwave incoming radiation (Rad).

Uncertainty for different climate variables can be computed as a range between the 5th and 95th percentiles and normalized by the total uncertainty to obtain a measure of the fractional contribution (Figure 5). This permits a relative cross-comparison of the primary uncertainty sources, even though the 5–95th percentile can only be approximated for the emission scenario uncertainty. The stochastic uncertainty overwhelms the other sources for mean and extreme precipitation, reaching almost 100% of the total uncertainty for the mid-century interval and roughly 70–80% for the end-of-the century period. For the mean, maximum and minimum daily temperatures, and mean relative humidity the three sources of uncertainty are comparable for the mid-century interval, while the scenario uncertainty accounts for approximately 80% of the total uncertainty at the end-of-the century. For solar radiation, the expected changes are very small and the three sources of uncertainty are comparable, especially for large lead-times. The arithmetic sum (Σ) of the three fractional uncertainties (5–95th percentile range) is close to 1.5 for precipitation and to 1.2 for temperature. These values are lower than the values expected for independent variables (Figure S5), supporting the expectation that the uncertainties cannot be assumed as independent and are rather positively correlated. There is a remarkable agreement in the results obtained for the three locations, suggesting that the presented results are unlikely to be a function of specific climatic conditions but rather represent a robust image of features of uncertainty partition at the local scale. Analyses for other stations in different climates will be important for a generalized understanding at the global scale but unlikely change the emerged property of uncertainty partition.

The assumption about the climate model inter-dependency has only a small influence on the results, while reducing the number of models increases climate model uncertainty (see detail in Figure S3). Climate model

limitations in simulating correctly precipitation patterns and capturing features of local climate are reflected in our analysis because they control climate model simulations and therefore the estimate of the uncertainty. The assumption of stationarity for each simulated period and internal static parameterizations of AWE-GEN are also influencing to some extent the final results. We contend that these "unaccounted uncertainties" (in our and in many other studies) are more likely to modify the climate change signal rather than considerably increase the total uncertainty and alter the relative contributions.

## 4. Discussion and Conclusions

Internal climate variability has been shown to be the dominant source of uncertainty in projections of mean and extreme precipitation not only for short lead-times (few decades), as currently acknowledged in literature [*Hawkins and Sutton*, 2011; *Trenberth*, 2012], but also for century distant projections, as already hinted by a regional study [*Hingray and Saïd*, 2014]. Differences from previous studies are expected because of the focus on small point-scales, the capability of our methodology to partition uncertainty sources without assuming them to be independent, and other assumptions, which are unavoidable in this type of study.

One apparent consequence is that the results appear to leave limited room for uncertainty reduction in precipitation projections even if methodologies and emission scenarios are significantly improved. Does the dominance of stochastic (irreducible) uncertainty suggest that improvements to climate models or higher resolution projections are unnecessary for local projections? Not at all. The improvement and availability of climate model realizations will still be fundamental to provide a more trustworthy climate change signal. The physical-basis of climate model simulations is in fact representing an important constraint, for instance potentially preserving the Clausius–Clapeyron relation for the scaling of short-term extreme precipitation with air temperature [e.g., *Ban et al*., 2014; *Westra et al*., 2014; *Molnar et al*., 2015]. As a matter of fact, when precipitation mean and extremes are considered: despite the large uncertainty dictated by the internal variability, the climate change signal can be detected in terms of the median. Thus, we claim that further model refinement should lead to identifying a more reliable median signal of the change, rather than in reduction of the spread of projection ensembles per se.

Does the dominance of irreducible uncertainty prevent us from making precise projections in terms of precipitation extremes at local scale? Very likely. Internal climate variability will remain even when a perfect model and an exact emission scenario would be used; therefore, issuing precise projections to serve the needs of ultimate users is not achievable. Frequency and/or intensity of extreme events will most likely increase [*Trenberth*, 2012; *Fischer et al*., 2013; *Westra et al*., 2014; *Molnar et al*., 2015] but we cannot precisely assess or predict where and by how much, because the signal to noise ratio is and will remain very small. This leads to another question: Does the lack of accurate and robust projections about changes in precipitation and extremes at local scale prevent us from making decisions in a changing climate? We think that such a statement would ignore decades of research dedicated to decision making under conditions of large uncertainty in various sectors, especially engineering [*Jordaan*, 2005; *Dessai et al*., 2009; *Hallegatte*, 2009]. While it would be impossible to provide precise information on local changes in precipitation sought by decision makers and stakeholders, we should not overlook that uncertainty is already dealt with in stochastic solutions for the current climate system and may suffice in many applications [*Lins and Cohn*, 2011; *Brown et al*., 2012; *Koutsoyiannis and Montanari*, 2015; *Montanari and Koutsoyiannis*, 2014; *Serinaldi and Kilsby*, 2015]. We argue that robust assessments of climate change scenarios are only possible taking into account internal climate variability and generally the largest range of possible trajectories in a probabilistic framework. In other words, a better description of uncertainty will help decision making, even when the latter can only use a subset of this information. Downscaling techniques similar to the one presented here or large multi-member ensembles of climate models perturbing initial conditions [*Deser et al*., 2012b, 2014; *Xie et al*., 2015] may represent the best approach. Using a single or few deterministic trajectories is a widespread approach in climate change projections and impact studies [e.g., *Seager et al*., 2007; *Elkin et al*., 2013], yet this could be very misleading because it neglects natural climate variability and could convey a false perception of certain information to end-users [*Deser et al*., 2012a; *Sexton and Harris*, 2015; *Thompson et al*., 2015]. For precipitation, we additionally suggest that impact studies which cannot afford elaborated and time-consuming analyses of climate model outputs should rely on proper accounting of historic climate variability, rather than selecting climate change signal from few subjectively chosen or available model

**Acknowledgments**
We thank two anonymous reviewers for their comments that contributed to improve the quality of the manuscript. We acknowledge the World Climate Research Programme's Working Group on Coupled Modelling, which is responsible for CMIP, and we thank the climate modeling groups (listed in Table S1 of this paper) for producing and making available their model output. For CMIP, the U.S. Department of Energy's Program for Climate Model Diagnosis and Intercomparison provides coordinating support and led development of software infrastructure in partnership with the Global Organization for Earth System Science Portals. A. Paschalis was supported by the SNSF (Grant P2EZP2-52244) and the Stavros Niarchos Foundation. V. Ivanov acknowledges the support of NSF Grant EAR 1151443.

runs. This study demonstrates that the historic internal variability for precipitation mean and extremes, if properly accounted for, is likely to be sufficient to cover a wide range of possible future trajectories.

## References


Anandhi, A., A. Frei, D. C. Pierson, E. M. Schneiderman, M. S. Zion, D. Lounsbury, and A. H. Matonse (2011), Examination of change factor methodologies for climate change impact assessment, *Water Resour. Res.*, *47*, W03501, doi:10.1029/2010WR009104.

Ban, N., J. Schmidli, and C. Schär (2014), Evaluation of the convection-resolving regional climate modeling approach in decade-long simulations, *J. Geophys. Res.*, *119*, 7889–7907, doi:10.1002/2014JD021478.

Bordoy, R., and P. Burlando (2014), Stochastic downscaling of precipitation to high-resolution scenarios in orographically complex regions: 1. Model evaluation, *Water Resour. Res.*, *50*, 540–561, doi:10.1002/2012WR013289.

Brown, C., Y. Ghile, M. Laverty, and K. Li (2012), Decision scaling: linking bottom-up vulnerability analysis with climate projections in the water sector, *Water Resour. Res.*, *48*, W09537, doi:10.1029/2011WR011212.

Caracciolo, D., L. V. Noto, E. Istanbulluoglu, S. Fatichi, and X. Zhou (2014), Climate change and ecotone boundaries: insights from a cellular automata ecohydrology model in a mediterranean catchment with topography controlled vegetation pattern, *Adv. Water Resour.*, *73*, 159–175, doi:10.1016/j.advwatres.2014.08.001.

Christensen, J. H., E. Kjellström, F. Giorgi, G. Lenderink, and M. Rummukainen (2010), Weight assignment in regional climate models, *Clim. Res.*, *44*, 179–194, doi:10.3354/cr00916.

Cowpertwait, P. S. P., V. Isham, and C. Onof (2007), Point process models of rainfall: developments for fine-scale structure, *Proc. R. Soc. Lond. A*, *463*(2086), 2569–2587, doi:10.1098/rspa.2007.1889.

Cox, P., and D. Stephenson (2007), A changing climate for prediction, *Science*, *317*(5835), 207–208, doi:10.1126/science.1145956.

Deser, C., R. Knutti, S. Solomon, and A. S. Phillips (2012a), Communication of the role of natural variability in future North American climate, *Nat. Clim. Change*, *2*, 775–779, doi:10.1038/nclimate1562.

Deser, C., A. Phillips, V. Bourdette, and H. Teng (2012b), Uncertainty in climate change projections: the role of internal variability, *Clim. Dyn.*, *38*, 527–546, doi:10.1007/s00382-010-0977-x.

Deser, C., A. S. Phillips, M. A. Alexander, and B. V. Smoliak (2014), Projecting north American climate over the next 50 years: uncertainty due to internal variability, *J. Clim.*, *27*, 2271–2296, doi:10.1175/jcli-d-13-00451.1.

Dessai, S., M. Hulme, R. Lempert, and R. Pielke Jr. (2009), Do we need better predictions to adapt to a changing climate? *Eos Trans. AGU*, *90*(13), 111, doi:10.1029/2009EO130003.

Elkin, C., A. G. Gutiérrez, S. Leuzinger, C. Manusch, C. Temperli, L. Rasche, and H. Bugmann (2013), A 2°C warmer world is not safe for ecosystem services in the European Alps, *Glob. Change Biol.*, *19*, 1827–1840, doi:10.1111/gcb.12156.

Fatichi, S., V. Y. Ivanov, and E. Caporali (2011), Simulation of future climate scenarios with a weather generator, *Adv. Water Resour.*, *34*, 448–467, doi:10.1016/j.advwatres.2010.12.013.

Fatichi, S., V. Y. Ivanov, and E. Caporali (2013), Assessment of a stochastic downscaling methodology in generating an ensemble of hourly future climate time series, *Clim. Dyn.*, *40*, 1841–1861, doi:10.1007/s00382-012-1627-2.

Fischer, E. M., U. Beyerle, and R. Knutti (2013), Robust spatially aggregated projections of climate extremes, *Nat. Clim. Change*, *3*, 1033–1038, doi:10.1038/nclimate2051.

Francipane, A., S. Fatichi, V. Y. Ivanov, and L. V. Noto (2015), Stochastic assessment of climate impacts on hydrology and geomorphology of semiarid headwater basins using a physically-based model, *J. Geophys. Res.: Earth Surf.*, *120*(3), 507–533, doi:10.1002/2014JF003232.

Giorgi, F. (2002), Dependence of the surface climate interannual variability on spatial scale, *Geophys. Res. Lett.*, *29*(23), 2101, doi:10.1029/2002GL016175.

Giorgi, F., and X. Bi (2009), Time of emergence (TOE) of GHG-forced precipitation change hot-spots, *Geophys. Res. Lett.*, *36*, L06709, doi:10.1029/2009GL037593.

Gueymard, C. A. (2008), REST2: high-performance solar radiation model for cloudless-sky irradiance illuminance and photosynthetically active radiation – validation with a benchmark dataset, *Solar Energy*, *82*, 272–285, doi:10.1016/j.solener.2007.04.008.

Hallegatte, S. (2009), Strategies to adapt to an uncertain climate change, *Global Environ. Change*, *19*, 240–247, doi:10.1016/j.gloenvcha.2008.12.003.

Hawkins, E., and R. Sutton (2009), The potential to narrow uncertainty in regional climate predictions, *Bull. Am. Meteorol. Soc.*, *90*, 1095–1107, doi:1010.1175/2009bams2607.1091.

Hawkins, E., and R. Sutton (2011), The potential to narrow uncertainty in projections of regional precipitation change, *Clim. Dyn.*, *37*, 407–418, doi:10.1007/s00382-010-0810-6.

Hawkins, E., and R. Sutton (2012), Time of emergence of climate signals, *Geophys. Res. Lett.*, *39*, L01702, doi:10.1029/2011GL050087.

Hingray, B., and M. Saïd (2014), Partitioning internal variability and model uncertainty components in a multimember multimodel ensemble of climate projections, *J. Clim.*, *27*, 6779–6798, doi:10.1175/jcli-d-13-00629.1.

Ivanov, V. Y., R. L. Bras, and D. C. Curtis (2007), A weather generator for hydrological, ecological, and agricultural applications, *Water Resour. Res.*, *43*, W10406, doi:10.1029/2006WR005364.

Jordaan, I. (2005), *Decisions Under Uncertainty: Probabilistic Analysis for Engineering Decisions*, Cambridge Univ. Press, Cambridge, UK.

Kendon, E. J., N. M. Roberts, C. A. Senior, and M. J. Roberts (2012), Realism of rainfall in a very high-resolution regional climate model, *J. Clim.*, *25*, 5791–5806, doi:10.1175/jcli-d-11-00562.1.

Kerr, R. A. (2011), Vital details of global warming are eluding forecasters, *Science*, *334*, 173–174, doi:10.1126/science.334.6053.173.

Kim, J., and V. Y. Ivanov (2015), A holistic, multi-scale dynamic downscaling framework for climate impact assessments and challenges of addressing finer-scale, *J. Hydrol.*, *522*, 645–660, doi:10.1016/j.jhydrol.2015.01.025.

Kim, J., V. Y. Ivanov, and S. Fatichi (2016), Climate change and uncertainty assessment over a hydroclimatic transect of Michigan, *Stochastic Environ. Res. Risk Assess.*, *30*(3), 923–944, doi:10.1007/s00477-015-1097-2.

Knutti, R. (2008), Should we believe model predictions of future climate change? *Philos. Trans. R. Soc. Lond. A*, *366*, 4647–4664, doi:10.1098/rsta.2008.0169.

Knutti, R., and J. Sedláček (2013), Robustness and uncertainties in the new CMIP5 climate model projections, *Nat. Clim. Change*, *3*, 369–373, doi:10.1038/nclimate1716.

Knutti, R., R. Furrer, C. Tebaldi, J. Cermak, and G. A. Meehl (2010), Challenges in combining projections from multiple climate models, *J. Clim.*, *23*, 2739–2758, doi:10.1175/2009jcli3361.1.

Knutti, R., D. Masson, and A. Gettelman (2013), Climate model genealogy: generation CMIP5 and how we got there, *Geophys. Res. Lett.*, *40*, 1194–1199, doi:10.1002/GRL.50256.

Koutsoyiannis, D. and A. Montanari (2015). Negligent killing of scientific concepts: the stationarity case, *Hydrol. Sci. J.*, *60*, 1174–1183, doi:10.1080/02626667.2014.959959.
Lins, H. F., and T. A. Cohn (2011), Stationarity: wanted dead or alive? *J. Am. Water Resour. Assoc.*, *47*, 475–480, doi:10.1111/j.1752-1688.2011.00542.x.
Little, C. M., R. M. Horton, R. E. Kopp, M. Oppenheimer, and S. Yip (2015), Uncertainty in twenty-first-century CMIP5 sea level projections, *J. Clim.*, *28*, 838–852, doi:10.1175/jcli-d-14-00453.1.
Marani, M., and S. Zanetti (2015), Longterm oscillations in rainfall extremes in a 268 year daily time series, *Water Resour. Res.*, *51*, 639–647, doi:10.1002/2014WR015885.
Maraun, D., et al. (2010), Precipitation downscaling under climate change: recent developments to bridge the gap between dynamical models and the end user, *Rev. Geophys.*, *48*, RG3003, doi:10.1029/2009RG000314.
Maslin, M., and P. Austin (2012), Climate models at their limit? *Nature*, *486*, 183–184, doi:10.1038/486183a.
Masson, D., and R. Knutti (2011), Climate model genealogy, *Geophys. Res. Lett.*, *38*, L08703, doi:10.1029/2011GL046864.
Molnar, P., S. Fatichi, L. Gaál, J. Szolgay, and P. Burlando (2015), Storm type effects on super Clausius–Clapeyron scaling of intense rainstorm properties with air temperature, *Hydrol. Earth Syst. Sci.*, *19*, 1753–1766, doi:10.5194/hess-19-1753-2015.
Montanari, A., and D. Koutsoyiannis (2014), Modeling and mitigating natural hazards: stationarity is immortal!, *Water Resour. Res.*, *50*(12), 9748–9756, doi:10.1002/2014WR016092.
Moss, R. H., et al. (2010), The next generation of scenarios for climate change research and assessment, *Nature*, *463*, 747–756, doi:10.1038/nature08823.
Murphy, J. M., D. M. H. Sexton, D. N. Barnett, G. S. Jones, M. J. Webb, M. Collins, and D. A. Stainforth (2004), Quantification of modelling uncertainties in a large ensemble of climate change simulations, *Nature*, *430*, 768–772, doi:10.1038/nature02771.
Orlowsky, B., and S. I. Seneviratne (2013), Elusive drought: uncertainty in observed trends and short- and long-term CMIP5 projections, *Hydrol. Earth Syst. Sci.*, *17*, 1765–1781, doi:10.5194/hess-17-1765-2013.
Papoulis, A. (1991), *Probability, Random Variables, and Stochastic Processes*, McGraw-Hill, New York.
Pappas, C., S. Fatichi, S. Leuzinger, A. Wolf, and P. Burlando (2013), Sensitivity analysis of a process-based ecosystem model: pinpointing parameterization and structural issues, *J. Geophys. Res.: Biogeosci.*, *118*(2), 505–528, doi:10.1002/JGRG.20035.
Paschalis, A., P. Molnar, S. Fatichi, and P. Burlando (2014), On temporal stochastic modeling of precipitation, nesting models across scales, *Adv. Water Resour.*, *63*, 152–166, doi:10.1016/j.advwatres.2013.11.006.
Peel, M. C., B. L. Finlayson, and T. A. McMahon (2007), Updated world map of the Köppen–Geiger climate classification, *Hydrol. Earth Syst. Sci.*, *11*, 1633–1644, doi:10.5194/hess-11-1633-2007.
Pennell, C., and T. Reichler (2010), On the effective number of climate models, *J. Clim.*, *24*, 2358–2367, doi:10.1175/2010jcli3814.1.
Rowell, D. P. (2012), Sources of uncertainty in future changes in local precipitation, *Clim. Dyn.*, *39*, 1929–1950, doi:10.1007/s00382-011-1210-2.
Saltelli, A., K. Chan, and M. Scott (2000), *Sensitivity Analysis*, Probability and Statistics Series, John Wiley and Sons, Chichester, UK.
Santer, B. D., et al. (2011), Separating signal and noise in atmospheric temperature changes: the importance of timescale, *J. Geophys. Res.*, *116*, D22105, doi:10.1029/2011JD016263.
Seager, R., et al. (2007), Model projections of an imminent transition to a more arid climate in Southwestern North America, *Science*, *316*, 1181–1184, doi:10.1126/science.1139601.
Serinaldi, F., and C. G. Kilsby (2015), Stationarity is undead: uncertainty dominates the distribution of extremes, *Adv. Water Resour.*, *77*, 17–36, doi:10.1016/j.advwatres.2014.12.013.
Sexton, D. M. H., and G. R. Harris (2015), The importance of including variability in climate change projections used for adaptation, *Nat. Clim. Change*, *5*, 931–936, doi:10.1038/nclimate2705.
Slingo, A. (1989), A GCM parameterization for the shortwave radiative properties of water clouds, *J. Atmos. Sci.*, *46*(10), 1419–1427, doi:10.1175/1520-0469(1989)046<1419:agpfts>2.0.CO;2.
Sobol, I. (1976), Uniformly distributed sequences with an additional uniform property, *USSR Comput. Math. Math. Phys.*, *16*(5), 236–242, doi:10.1016/0041-5553(76)90154-3.
Stephens, G. L. (1978), Radiation profiles in extended water clouds: 2. Parameterization schemes, *J. Atmos. Sci.*, *35*(11), 2123–2132, doi:10.1175/1520-0469(1978)035<2123:rpiewc>2.0.CO;2.
Taylor, K. E., R. J. Stouffer, and G. A. Meehl (2012), An overview of CMIP5 and the experiment design, *Bull. Am. Meteorol. Soc.*, *93*(4), 485–498, doi:10.1175/bams-d-11-00094.1.
Tebaldi, C., L. Mearns, D. Nychka, and R. Smith (2004), Regional probabilities of precipitation change: a Bayesian analysis of multimodel simulations, *Geophys. Res. Lett.*, *31*, L24213, doi:10.1029/2004GL021276.
Tebaldi, C., R. L. Smith, D. Nychka, and L. O. Mearns (2005), Quantifying uncertainty in projections of regional climate change: a Bayesian approach to the analysis of multi-model ensembles, *J. Clim.*, *18*, 1524–1540, doi:10.1175/jcli3363.1.
Thompson, D. W. J., E. A. Barnes, C. Deser, W. E. Foust, and A. S. Phillips (2015), Quantifying the role of internal climate variability in future climate trends, *J. Clim.*, *28*, 6443–6455, doi:10.1175/jcli-d-14-00830.1.
Trenberth, K. E. (2012), Framing the way to relate climate extremes to climate change, *Clim. Change*, *115*(2), 283–290, doi:10.1007/s10584-012-0441-5.
Weigel, A. P., R. Knutti, M. A. Liniger, and C. Appenzeller (2010), Risks of model weighting in multimodel climate projections, *J. Clim.*, *23*, 4175–4190, doi:10.1175/2010jcli3594.1.
Westra, S., H. J. Fowler, J. P. Evans, L. V. Alexander, P. Berg, F. Johnson, E. J. Kendon, G. Lenderink, and N. M. Roberts (2014), Future changes to the intensity and frequency of short-duration extreme rainfall, *Rev. Geophys.*, *52*, 522–555, doi:10.1002/2014RG000464.
Xie, S.-P., et al. (2015), Towards predictive understanding of regional climate change, *Nat. Clim. Change*, *5*, 921–930, doi:10.1038/nclimate2689.
Yip, S., C. A. T. Ferro, D. B. Stephenson, and E. Hawkins (2011), A simple, coherent framework for partitioning uncertainty in climate predictions, *J. Clim.*, *24*, 4634–4643, doi:10.1175/2011jcli4085.1.